Free Radical Biology and Medicine 227 (2025) 117–128

Contents lists available at ScienceDirect

Free Radical Biology and Medicine

journal homepage: www.elsevier.com/locate/freeradbiomed

Molecular evolution of ovothiol biosynthesis in animal life reveals diversity of the natural antioxidant ovothiols in Cnidaria

Annalisa Zuccarotto [a,b], Marco Sollitto [c,d], Lucas Leclère [e], Lucia Panzella [f], Marco Gerdol [b,c], Serena Leone [b], Immacolata Castellano [a,b,*]

[a] Department of Molecular Medicine and Medical Biotechnology, University of Naples Federico II, 80131, Naples, Italy
[b] Department of Biology and Evolution of Marine Organisms, Stazione Zoologica Anton Dohrn, Villa Comunale, 80121, Naples, Italy
[c] Department of Life Sciences, University of Trieste, 34128, Trieste, Italy
[d] Department of Biology, University of Florence, 50019, Sesto Fiorentino, FI, Italy
[e] Sorbonne Université, CNRS, Biologie Intégrative des Organismes Marins (BIOM), Banyuls-sur-Mer, France
[f] Department of Chemical Sciences, University of Naples "Federico II", I-80126 Naples, Italy

ARTICLE INFO

Keywords:
Ovothiol
Antioxidants
Glutathione
Cnidaria
Corals
Redox evolution

ABSTRACT

Sulfoxide synthase OvoA is the key enzyme involved in the biosynthesis of ovothiols (OSHs), secondary metabolites endowed with unique antioxidant properties. Understanding the evolution of such enzymes and the diversity of their metabolites should reveal fundamental mechanisms governing redox signaling and environmental adaptation. "Early-branching" animals such as Cnidaria display unique molecular diversity and symbiotic relationships responsible for the biosynthesis of natural products, however, they have been neglected in previous research on antioxidants and OSHs.

In this work, we have integrated genome and transcriptome mining with biochemical analyses to study the evolution and diversification of OSHs biosynthesis in cnidarians. By tracing the history of the *ovoA* gene, we inferred its loss in the latest common ancestor of Medusozoa, followed by the acquisition of a unique *ovoB/ovoA* chimaeric gene in Hydrozoa, likely through a horizontal gene transfer from dinoflagellate donors. While Anthozoa (corals and anemones), bearing canonical *ovoA* genes, produced a striking variety of OSHs (A, B, and C), the multifunctional enzyme in Hydrozoa was related to OSH B biosynthesis, as shown in *Clytia hemisphaerica.* Surprisingly, the *ovoA*-lacking jellyfish *Aurelia aurita* and *Pelagia noctiluca* also displayed OSHs, and we provided evidence of their incorporation from external sources. Finally, transcriptome mining revealed *ovoA* conserved expression pattern during larval development from Cnidaria to more evolved organisms and its regulation by external stimuli, such as UV exposure. The results of our study shed light on the origin and diversification of OSH biosynthesis in basal animals and highlight the importance of redox-active molecules from ancient metazoans as cnidarians to vertebrates.

1. Introduction

The animals belonging to the phylum Cnidaria have always captivated scientists and artists due to their astonishing diversity in morphology, colors and beauty of life forms. Cnidaria includes two major clades of organisms, *i.e.* Anthozoa (corals, sea anemones, and sea pens) and Medusozoa (mainly jellyfish) distinguished by spectacular life cycles [1–3]. While Anthozoans' life cycle involves free-swimming planulae, developing into sessile polyps, without a medusa stage [4], most Medusozoa alternate the asexual polyps and sexually mature medusa stages [4]. Cnidaria are significant for evolutionary studies due to their key position in the metazoan tree of life, as a sister group to Bilateria, with whom they share many conserved genes with ancient origin [5,6]. They are also studied for sensitivity to anthropogenic pressure and the extraordinary endosymbiotic relationships with bacteria or photosynthetic dinoflagellate algae [7]. Cnidarian-associated microbiomes have long been considered the main entities responsible for the biosynthesis of many bioactive molecules, including several antioxidants [8,9]. However, recent studies have challenged this view, showing that cnidarian hosts also possess the biosynthetic capacity to synthesize several secondary metabolites with potential bioactivity [10]. In this regard, we have recently reported that most Anthozoans

* Corresponding author. Department of Molecular Medicine and Medical Biotechnology, University of Naples Federico II, 80131, Naples, Italy.
E-mail address: immacolata.castellano@unina.it (I. Castellano).

https://doi.org/10.1016/j.freeradbiomed.2024.11.037
Received 21 August 2024; Received in revised form 31 October 2024; Accepted 20 November 2024
Available online 29 November 2024
0891-5849/© 2024 The Authors. Published by Elsevier Inc. This is an open access article under the CC BY-NC-ND license (http://creativecommons.org/licenses/by-nc-nd/4.0/).

possess the genes responsible for the production of ovothiols (OSHs), a class of sulfur-containing histidine derivatives [11], found in nature in three different methylated forms, OSH A, B, and C, in the eggs and biological fluids of marine invertebrates (echinoderms and mollusks), some protozoa (Trypanosoma) and protists (microalgae) [12–15].

The main enzymes responsible for sulfur-containing histidine production are sulfoxide synthases, which perform the oxidative C-S coupling, leading to the insertion of a sulfur atom on the imidazole ring of histidine [16]. The only two sulfoxide synthases known to catalyze this type of reaction are EgtB, involved in the biosynthesis of the trimethyl-2-thio-histidine, ergothioneine (ERG), mainly in fungi and cyanobacteria [17,18], and the 5-histidylcysteine sulfoxide synthase OvoA, involved in the biosynthesis of OSHs [19]. OvoA is a bifunctional protein comprising a non-heme iron-dependent sulfoxide synthase in the N-terminal region and a S-adenosyl methionine-dependent (SAM) methyltransferase at the C-terminus [19]. The N-terminal domain of OvoA, in the presence of oxygen, catalyzes the formation of the 5-histidyl-cysteine sulfoxide conjugate using cysteine and histidine as substrates. Subsequently, the enzyme pyridoxal phosphate (PLP)-dependent lyase (OvoB) cleaves this intermediate to produce 5-thiohistidine [20]. Finally, the SAM domain of OvoA catalyzes the methylation at the imidazole ring to produce OSH A. OSH B and OSH C differ from OSH A due to the presence of additional methylation at the lateral chain of histidine, which is catalyzed by unknown enzymes. The three-dimensional structures of bacterial OvoA and OvoB from *Hydrogenimonas thermophila* and *Erwinia tasmaniensis*, respectively, have been only recently determined [20,21]. While OvoB-like homologous enzymes have not been unambiguously identified in animals, *ovoA* orthologous genes are present in several metazoans [22], displaying a patchy distribution that highlights a complex evolutionary history [11]. Although *ovoA* has an ancient origin, which can be traced back to the latest common ancestor of Choanozoa, its orthologs were lost in several major extant taxa, like Ecdysozoa and Vertebrata, or secondarily re-acquired through horizontal gene transfer (HGT) in others, such as hydrozoans and bdelloid rotifers [11]. The reasons underlying the loss of *ovoA* genes in some phyla and their retention and diversification in others remain obscure. However, OSHs probably represent the most intriguing marine sulfur-containing secondary metabolites due to their unique redox properties. The peculiar position of the thiol group on the imidazole ring of OSH results in strikingly different chemical and biological properties. In fact, the p*K*a of OSH's thiol group (~1.4) is significantly lower compared to that of other natural thiols, including glutathione GSH (usually within a range of 7.0–9.0) [14]. Under physiological conditions, OSH A exists predominantly in the thiolate form and functions as a potent radical and peroxide scavenger [23,24]. The antioxidant action of OSH A generates OSH A disulfide, which is then reduced by intracellular GSH. Therefore, the OSH/GSH system has been proposed to protect sea urchin eggs against fertilization-induced oxidative stress [25,26]. In contrast, ERG is mainly found in its thione form in physiological conditions, and cannot produce a disulfide [18], however, it can efficiently scavenge reactive oxygen species (ROS) and exerts a protective action also in several human pathologies, such as neurodegenerative diseases and cardiovascular disorders [27], to the point that it has been recently labeled as a "longevity vitamin" [28]. Comparative studies on OSHs have long been neglected, being at their early stages. New evidence suggests biological and ecological roles of OSH might be more complex than originally thought, going far beyond simple cellular protection [14]. Indeed, OSH A can be part of more complex structures in the sea star *Dermasteria imbricata* [29], in the sponge *Latrunculia brevis* [30], and in the venom of the cone snail, *Conus imperialis* [31]. Recent studies have also reported that OSH A exerts protective and anti-inflammatory properties in human models of endothelial dysfunction, liver fibrosis, and skin inflammation, through the modulation of ROS, NO signaling, and GSH metabolism [32–35]. Overall, these findings suggest that OSHs are involved in fine regulation of redox-sensitive pathways, and have the potential to ameliorate oxidative stress-related pathologies [32,33].

The present manuscript integrates genome and transcriptome data mining with biochemical analyses to study the evolution and diversification of the enzymes involved in OSHs biosynthesis in Cnidaria. The elucidation of the evolutionary origins of the canonical *ovoA* genes of Anthozoa and the unusual chimaeric *ovoB/ovoA* genes of Hydrozoa, together with the identification of diverse OSHs forms in different cnidarian species by HPLC and LC-MS highlighted extraordinary molecular and metabolic complexity in this basally-branching animal phylum. This work reveals, for the first time, a new biosynthetic capacity for cnidarian hosts, providing new insights into the evolution of sulfur redox homeostasis in animals and unlocking the repertoire of bioactive antioxidant molecules from these organisms.

2. Results

2.1. Evolutionary history of OvoA: focus on Cnidaria

The considerable increase in sequenced genomes in the phylum Cnidaria prompted a much more detailed atlas of genuine *ovoA* orthologous genes in these organisms, compared to the previous study [11]. First, we confirmed the widespread presence of *ovoA* genes in all anthozoans, both belonging to Hexacorallia and Octocorallia. All anthozoan sequences are orthologous to those found in the other metazoans (except for the genes of the bdelloid rotifers), as they fall with a high probability within the same clade (clade I, see Fig. 1A) according to phylogenetic inference analysis. Second, we confirmed the previously hypothesized absence of *ovoA* genes in the genome of three medusozoan classes, i.e. Cubozoa, Scyphozoa, and Staurozoa, as well as in the obligate cnidarian parasites of the Myxozoa subphylum (see Fig. 1B). The updated comparative genomics analysis clarified the distribution of the sequences found in the class Hydrozoa, which display a peculiar structural organization, unique in metazoan evolution (discussed in detail below), and belonging to clade II (see Fig. 1A), along with those of many alveolates and photosynthetic protists. The analysis of the recently released high-quality hydrozoan genome assemblies [3,36–41] highlighted the presence of a single *ovoB/ovoA* chimaeric gene copy in members of the two subclasses Hydroidolina and Trachylinae, living in both marine and freshwater environments. A comprehensive list of all detected anthozoan and hydrozoan OSH biosynthetic gene sequences in available genomes and transcriptomes is reported in SI Table S1.

2.2. OSH biosynthetic genes and protein structure domains in Cnidaria

To better characterize the diversification of OSH biosynthesis in cnidarians, we compared the structure of *ovoA* genes and encoded proteins within this phylum. The *ovoA* gene of all anthozoan species displayed a number of exons (approximately 17–20), most of which had highly conserved boundaries, shared with the *ovoA* orthologues of other metazoan phyla [11]. The encoded proteins had a canonical domain organization: a DinB superfamily domain, with the highly conserved iron-binding motif (HX_3HXE) in the N-terminal region; a formyl-glycine FGE-sulfatase domain, with the conserved tyrosine (*Et*Tyr417), essential for sulfoxide synthase catalytic activity [43] and the residues responsible for binding to cysteine and histidine [21,22]; a single SAM-transferase domain in the C-terminal region (SI Fig. 1). On the other hand, hydrozoan genes had a different, more complex architecture, characterized by the presence of an additional N-terminal PLP dependent β-lyase domain, similar to OvoB, fused at its C-terminus with an OvoA-like protein [11]. Therefore, these chimaeric hydrozoan sequences may combine the activities of the two enzymes involved in OSH biosynthesis within the same polypeptide. Moreover, hydrozoan genes contained two C-terminal SAM domains. Consistently with the remarkable structural differences observed at the protein level with anthozoans, hydrozoan OvoA sequences were placed with high confidence in a different phylogenetic clade (i.e. clade II, Fig. 1A), and displayed a

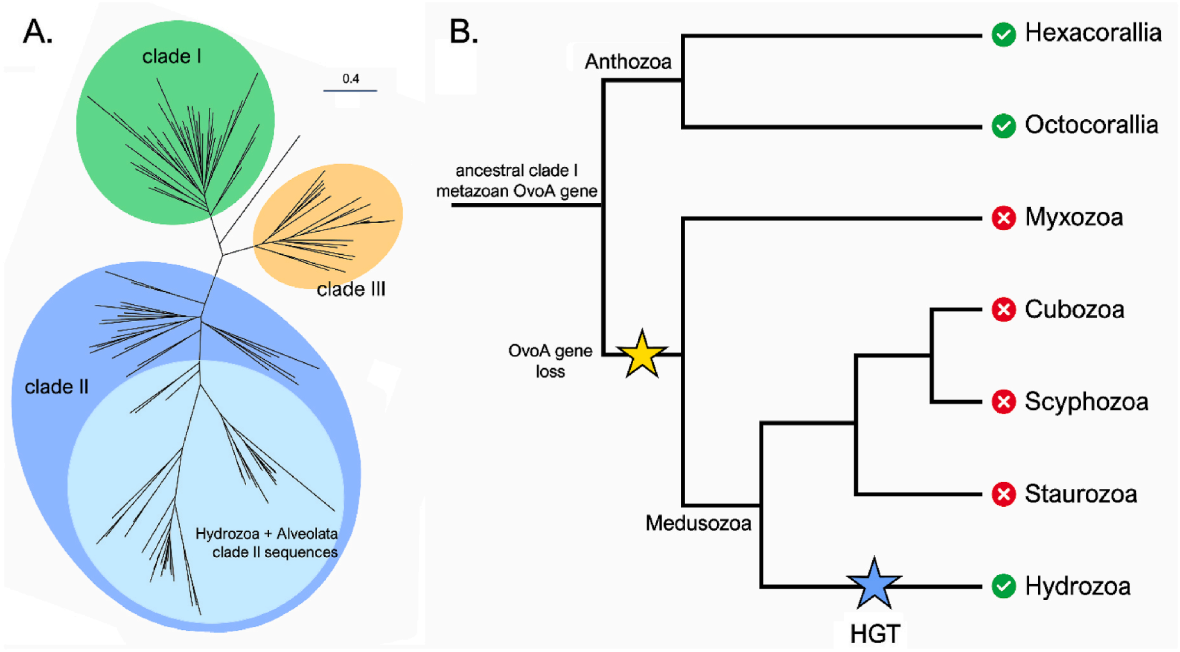

Fig. 1. A) Evolutionary relationship among representative OvoA sequences from animals, bacteria, and protists, and positioning of the hydrozoan HGT event. The evolutionary relationship among all OvoA sequences was inferred using Maximum Likelihood inference and an LG + I + G model of molecular evolution. The three main sequence clades previously identified by Ref. [11] are indicated with different colors. The subgroup of clade II sequences belonging to Hydrozoa and Alveolata is marked in light blue. All dichotomic nodes are supported by posterior probability >0.5 B) Schematic reconstruction of OvoA evolution in Cnidaria phylum, inferring the loss of a clade I *ovoA* gene in the common ancestor of Myxozoa and Medusozoa, followed by the reacquisition of clade II *ovoB/ovoA* chimaeric gene in Hydrozoa by HGT. The evolutionary relationships among the different cnidarian subclasses are based on a previous study [42]. (For interpretation of the references to color in this figure legend, the reader is referred to the Web version of this article.)

variable gene architecture, with 4 (in *Hydra* spp. and *Candelabrum coksii*) to 17 (in *C. hemisphaerica*) exons, and a few conserved introns that were not shared with any other metazoan *ovoA* gene. In detail, the OvoB-like domain, which preserves the residues responsible for PLP binding and the key lysine (K240 in *Et*OvoB) responsible for lyase activity, was entirely encoded by the first large 5' exon in *Hydra* spp., *Turritopsis* spp. and *C cocksii*, split between exon 1 and 2 in *Hydractinia* spp., and placed between exons 2 and 7 in *C. hemisphaerica* (Fig. 2A). In *Hydra* spp., *Turritopsis* spp. and *C. cocksii*, the first exon encoded both for the OvoB-like and for the DinB and FGE sulfatase domains of OvoA [11], while the two SAM domains were encoded by subsequent exons. This relatively simple gene architecture was highly modified in other hydrozoan species, such as *Hydractinia* spp. and *C. hemisphaerica*, where multiple additional introns were acquired (Fig. 2A).

To highlight structural and functional novelties in hydrozoans, we predicted the complete three-dimensional structure of the multidomain OvoB/OvoA protein from the marine *C. hemisphaerica* (*Ch*OvoBA), with AlphaFold2 [44,45]. The model was predicted with high confidence, with an average pLDDT higher than 90 for most of the globular regions (Fig. 2B). Notably, three segments characterized by low pLDDT (<40) were detected: 1) in the OvoB region (residues 397–449); 2) between the DinB and FGE domains (residues 648–658); 3) in the segment connecting the two SAM domains (residues 1191–1212). This is most likely due to regions characterized by low coverage in the multiple sequence alignments, or by actual disordered regions, with specific functional relevance [46]. The analysis of the Predicted Aligned Error (PAE) plot (Fig. 2C), which provides a measure of the reliability of the reciprocal orientation of the individual domains, indicated two independent structural blocks: the first one encompassing the N-terminal OvoB, DinB and FGE domains, that appear therefore stably structured and oriented; the second one comprising the two SAM domains. The relative position of these two structural conglomerates in the model seems instead more flexible. The only structure of OvoA enzyme available in the PDB database from the thermophilic microorganism *H. thermophila* ($OvoA_{Ht2}$, PDB 8KHQ) shows that the functional enzyme is a homodimer assembled through an antiparallel β-sheet formed by the outermost strand in the SAM domain of each monomer [21]. Interestingly, in the model of *Ch*OvoBA the same architecture would be assembled through the interaction of the two SAM domains within a single monomer, preventing the dimerization of the protein similarly (Fig. 2B; SI Fig. 2). A comparison of the active site of *Ch*OvoBA and $OvoA_{Ht2}$ highlights the conservation of the position of all the residues essential for the catalytic activity (Fig. 2D). At the N-terminal of *Ch*OvoBA, the OvoB-like domain presents the typical fold of a PLP-dependent lyase. This portion has very low sequence homology (13.4 % identity) with OvoB from *E. tasmaniensis* ($OvoB_{Eta}$, PDB 5Z0Q). PLP-dependent enzymes, including $OvoB_{Eta}$, are usually dimeric and the catalysis takes place at the interface between the two subunits [47]. The model of the dimer for *Ch*OvoB was also obtained with AlphaFold2 and, despite its recognizable fold, it appeared quite different from $OvoB_{Eta}$, with the most pronounced differences localized right at the interface between the subunits (SI Fig. 3). This, together with the low sequence homology with $OvoB_{Eta}$, allowed us to identify only a few of the residues known to mediate PLP binding and catalysis, *i.e.*, K259, Y146 and D231 (Fig. 2E). The other residues composing the active site could not be unequivocally identified neither by sequence comparison nor by structure superposition. Based on this observation, *Ch*OvoBA is likely a dimeric protein, in which the two monomers interact through the OvoB-like domain. Thanks to the recent introduction of AlphaFold3 [48], we were able to model also the dimeric assembly with reasonable confidence (Fig. 2F). This presents a horseshoe structure in which, as predicted based on the PAE plot (SI Fig. 4), the SAM domains of each subunit are more flexible compared to the rest of the structure. This may facilitate the methylation steps during the biosynthetic process.

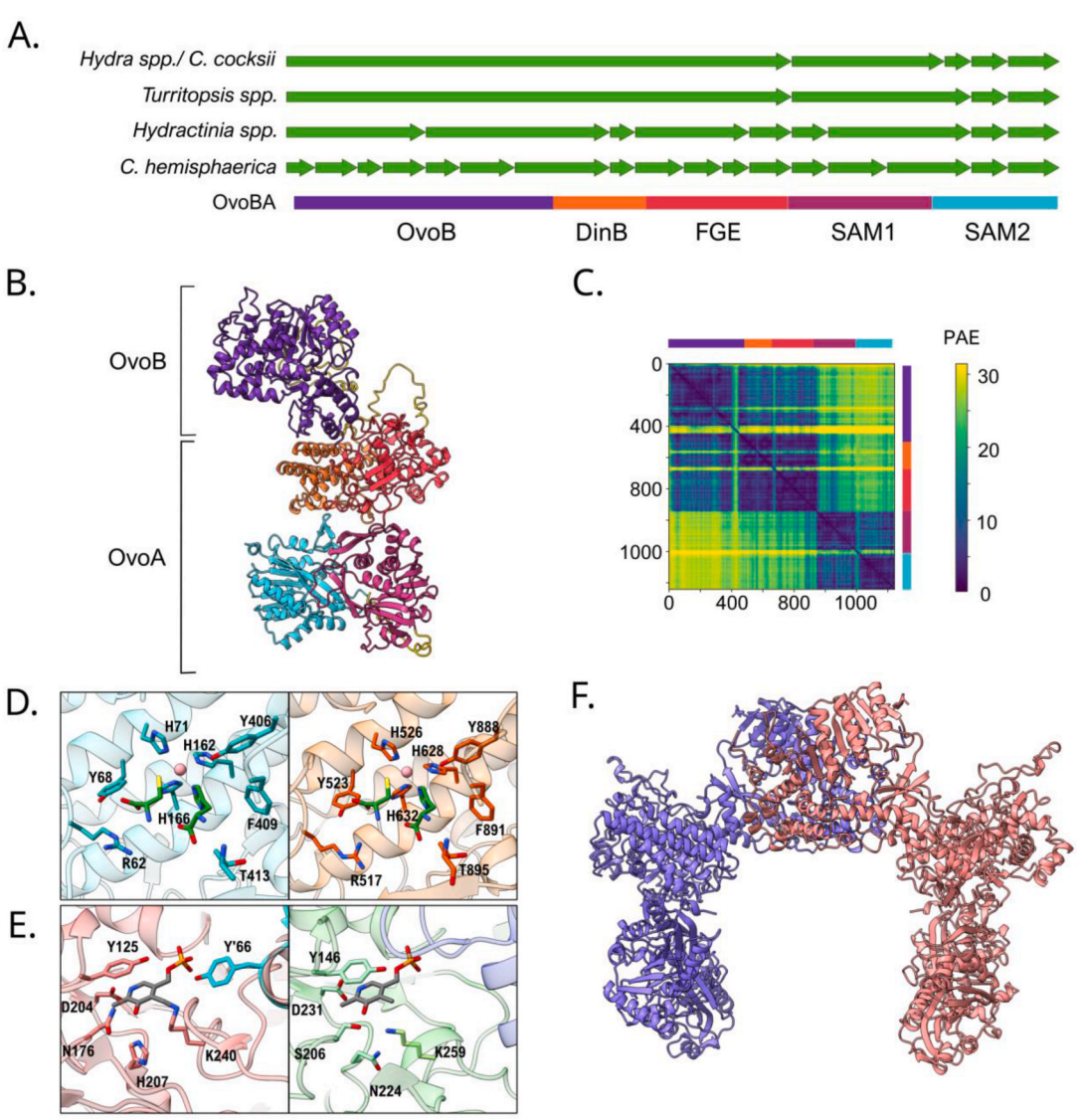

Fig. 2. A) Examples of diversified exons organization in representative *ovoB-ovoA* chimaeric genes from hydrozoans and comparison with the individual domains within the protein structure (colored segments on the bottom). B) AlphaFold2 model of *Ch*OvoBA protein. The two enzymatic functions are highlighted and the structural domains are colour coded according to their succession within the sequence. The regions that were modeled with low confidence are depicted in yellow. C) Map of the PAE for the model of the multidomain *Ch*OvoBA, highlighting the relative positions of the different domains. For clarity, the protein sequence is sketched along the axes. Lower values (blue) indicate a more compact arrangement and support the interaction between the OvoB-DinB-FGE domain, whereas a second structural block is constituted by the two interacting SAM domains. D) Comparison of the catalytic site of $OvoA_{Ht2}$ (8KHQ, light blue, left) and the corresponding portion of *Ch*OvoBA (orange, right). The metal coordination site and the relevant catalytic residues are highlighted. E) Comparison of the PLP binding site in $OvoB_{Eta}$ (5Z0Q, pink, left) and *Ch*OvoBA (green, right). F) AlphaFold3 predicted structure of the functional dimer of ChOvoBA. The two monomers are indicated in different colors. (For interpretation of the references to color in this figure legend, the reader is referred to the Web version of this article.)

2.3. Hydrozoan chimaeric genes likely derive from intracellular dinoflagellate parasites

Although different lines of evidence point to an independent evolutionary origin for the chimaeric hyrozoan *ovoA* genes, compared with all the other metazoan sequences, both the timing and the mechanisms underpinning the acquisition of these sequence in the latest common ancestor of all extant hydrozoan species (light blue clade, Fig. 3) require further investigation. Here we report for the first time the presence of homologous sequences in the genomes of parasitic dinoflagellates belonging to the family Syndiniales, i.e *Amoebophyra* sp. A120 [49] and *Amoebophrya ceratii* [50], as well as in a metagenome-assembled genome [51] that may also derive from an uncharacterized *Amoebophrya*-related organism. The *OvoB/OvoA* chimaeric sequences from Syndiniales formed a sister clade to those of Hydrozoa (red clade, Fig. 3), supporting with high confidence (posterior probability = 1) their monophyletic origin. Although a few additional sequences were identified in the transcriptome assemblies of other free-living dinoflagellate species, as well as in a few species of unicellular algae and flagellates with sparse phylogenetic placement (green clade, Fig. 3), their presence could not be confirmed at the genomic level in any of these organisms. In light of the parasitic lifestyle of Syndiniales and their adaptation to a broad range of hosts, the most parsimonious interpretation is that these transcripts are contaminations from intracellular parasites rather than endogenous host gene products. Regardless of their taxonomic origins, phylogenetic inference strongly supports (i.e. posterior probability = 1, Fig. 3) the monophyly of all chimaeric *OvoB/OvoA* sequences. Prior to this work, the clade II OvoA canonical sequence (i.e lacking the OvoB-like domain) most closely related with the hydrozoan sequences had been identified in the alveolate *V. brassicaformis*. Here we can extend similar findings to

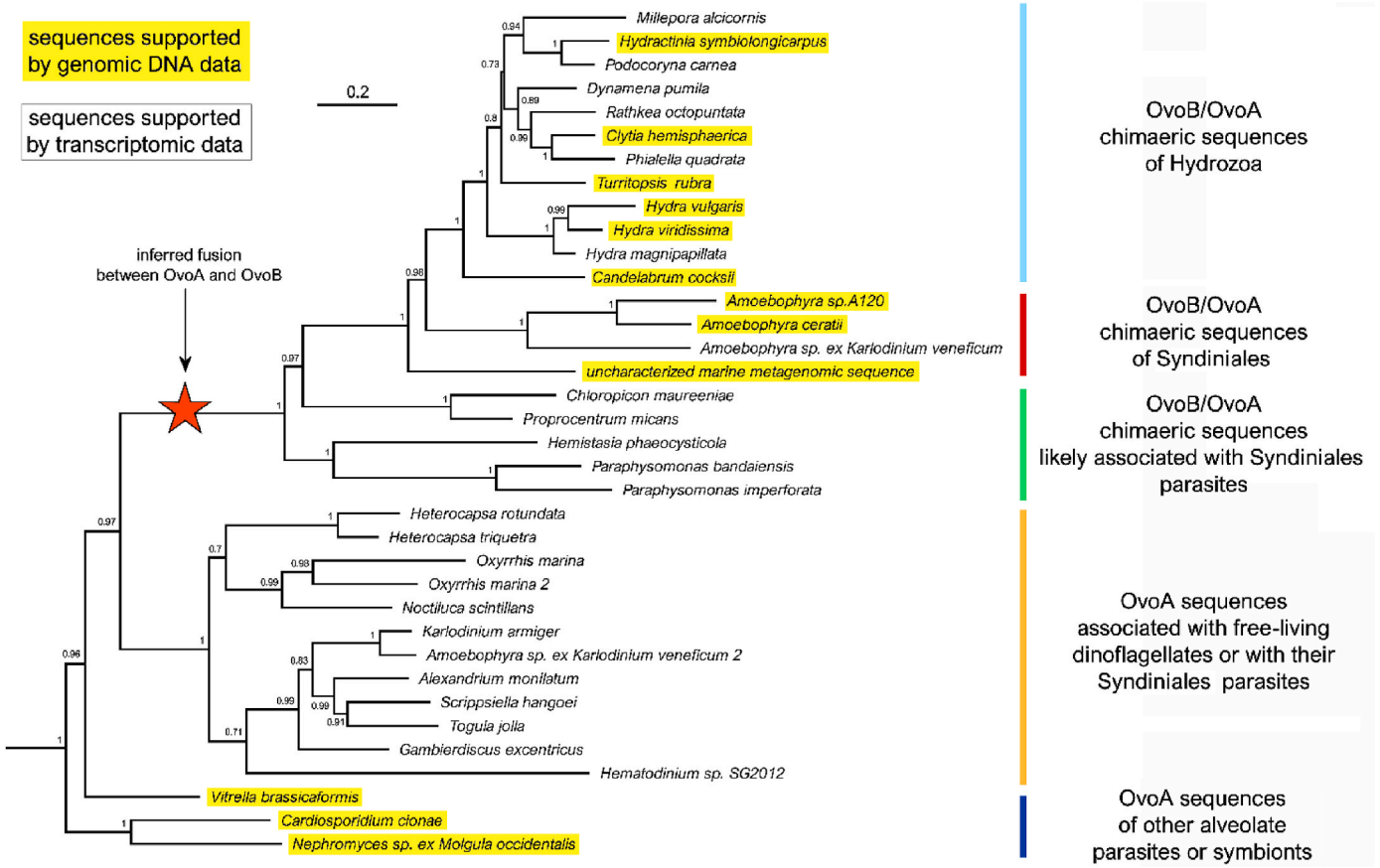

Fig. 3. Zoomed-in view of the tree branch marked in light blue in Fig. 1A), showing the details of the evolutionary relationships among the sequences relevant for the hydrozoan HGT event. The sequences supported by genomic data, highlighted in yellow, have a certain taxonomic assignment. In contrast, those obtained from transcriptome assemblies may derive from associated parasites or symbionts, as discussed in the main text. The numbers shown close to each tree node indicate posterior probability support values. (For interpretation of the references to color in this figure legend, the reader is referred to the Web version of this article.)

the genomes of the apicomplexans *Nephromyces* sp. ex *Molgula occidentalis* and *Cardiosporidium cionae* (dark blue clade, Fig. 3), which are both associated with tunicate hosts [52,53], further identifying a large monophyletic clade of similar sequences in the transcriptomes of parasitic Syndiniales (e.g. *Hematodinium* and *Amoebophrya* spp.) as well as in the transcriptome of other free-living dinoflagellates, where they may either represent genuine endogenous gene products or transcripts expressed by their parasites (orange clade, Fig. 3). These observations support the presence of clade II *ovoA* genes phylogenetically related with those of Hydrozoa and *Amoebophrya*, but lacking an OvoB-like N-terminal domain, in several distantly related alveolates. As of note, some of these species also have *ovoB*-like genes, which supports the hypothesis that *ovoA* and *ovoB*, present as two distinct gene products in several Alveolata, were fused at some point during the evolution of Syndiniales, leading to the chimaeric genes observed in *Amoebophrya* (red star, Fig. 3). Overall, these findings support an ancestral origin of the hydrozoan chimaeric sequences by HGT from a symbiotic dinoflagellate harboring an intracellular parasite belonging to Syndiniales.

2.4. Identification and characterization of ovothiols in Cnidaria

We aimed to investigate whether the highlighted evolutionary differences between anthozoan and hydrozoan OvoA sequences corresponded to a diversification in the composition of the thiol pool in several representative species from different classes of Cnidaria. Cellular thiols were identified employing HPLC and LC-MS analyses in three anthozoan and three medusozoan species: the octocoral *Eunicella singularis,* the two Hexacorallia *Astroides calycularis* (Scleractinia) and *Actinia equina* (Actinaria), the two scyphozoans *Aurelia aurita* and *Pelagia noctiluca* and the hydrozoan *Clytia hemisphaerica*. Analyses were performed by HPLC analysis and compared with available standards after extraction from lyophilized specimens and derivatization with 4-bromomethyl-7-methoxycoumarin (BMC). This analysis was further complemented by LC-MS runs, to resolve ambiguities. Among Anthozoa (Fig. 4A), we detected the presence of OSH A ($[M+H]^+ = 390$ *m/z*) as predominant species in the octocoral *E. singularis* and in low abundance in the hexacoral scleractinia *A. calycularis.* Notably, in *E. singularis* traces of OSH B ($[M+H]^+ = 404$ *m/z*) were detectable only by the LC-MS analysis), whereas no traces of GSH were observed in this species. However, low amount of GSH was detected in *A. calycularis* ($[M+H]^+ = 496$ *m/z*). On the other hand, the hexacoral actinaria *A. equina* contained exclusively OSH C, as confirmed by the occurrence of a compound characterized by a pseudomolecular ion peak $[M+H]^+$ at 418 *m/z*, corresponding to the BMC adduct of OSH C, in the LC-MS profile. OSH C and GSH were present in comparable amounts in this species, with a molar [OSH]/[GSH] ratio equal to 0.86. In the analysis of the extracts from colorful Anthozoa, several peaks were visible, but not all of them could be identified and ascribed to known cellular thiols. This is possibly due to the abundance of pigments that were likely retained throughout the derivatization procedure. However, no ERG analogues were detected in these animals.

Within Medusozoa, analyses on the scyphozoans *A. aurita* polyps and *P. noctiluca* young medusae highlighted the presence of GSH as the main cellular thiol. No trace of OSHs was detected in *A. aurita* polyps (Fig. 4B; SI Fig. 5), as expected based on the observed lack of *ovoA* gene in this lineage. Surprisingly, when analysing samples from adult jellyfish *P. noctiluca*, fed with mollusks, we could also detect the presence of OSH A and small traces of OSH B (Fig. 4B; SI Fig. 5). Adult jellyfish of

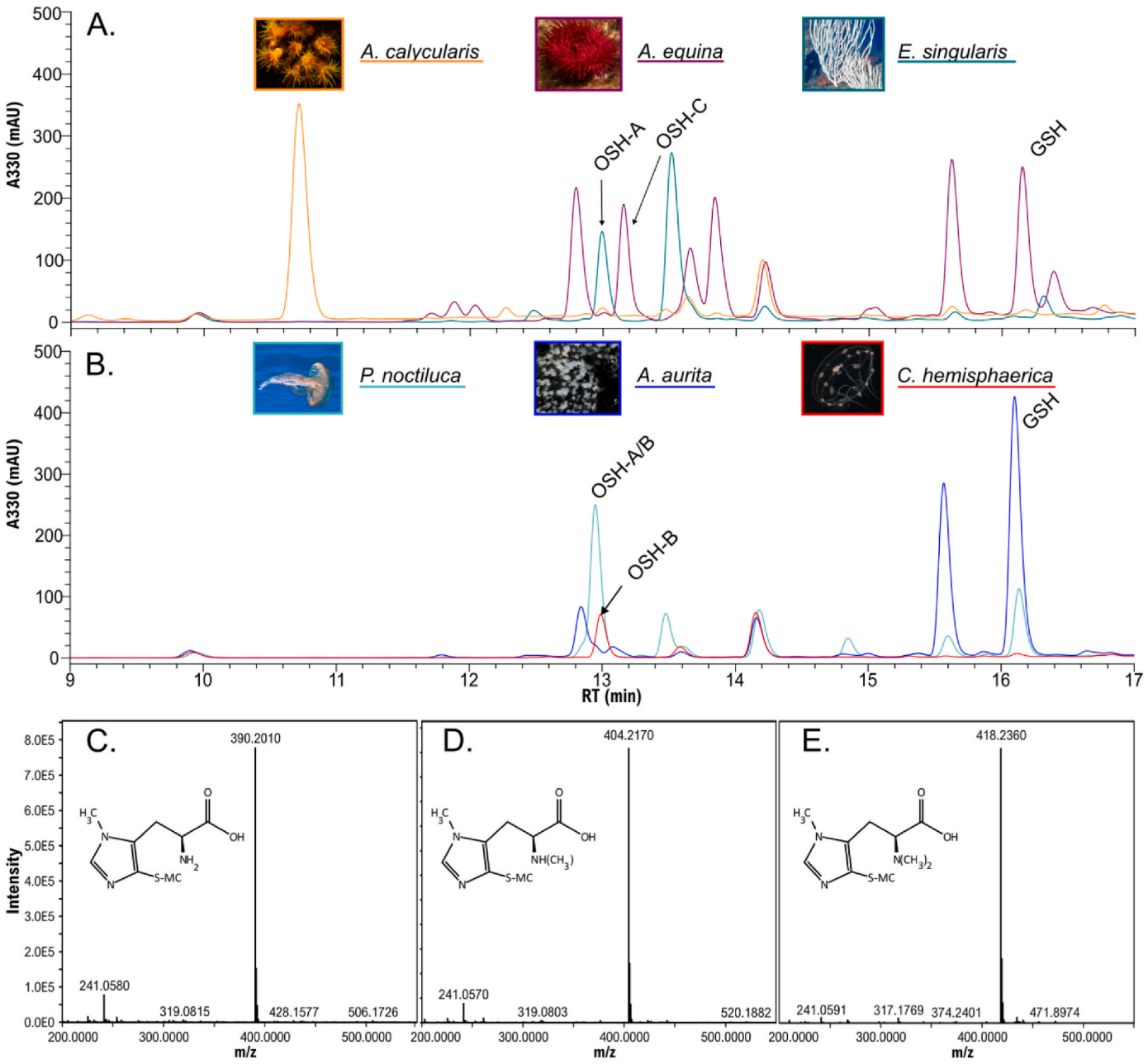

Fig. 4. Analysis of the cellular thiols in different Cnidaria: A) Comparison of the HPLC profiles from Anthozoa: *A. calycularis* (yellow), *A. equina* (pink) and *E. singularis* (light blue). B) Comparison of the HPLC profiles from Medusozoa: *P. noctiluca* adults (light blue), *A. aurita* polyps (dark blue) and *C. hemisphaerica* (red). C,D,E). MS spectra of OSH A (*E. singularis*), OSH B (*C. hemisphaerica*), and OSH C (*A. equina*), respectively. (For interpretation of the references to color in this figure legend, the reader is referred to the Web version of this article.)

A. aurita, fed with *Artemia salina* confirmed also in this species the presence of OSH A, suggesting that Medusozoa can acquire OSHs from diet (SI Fig. 5). Finally, OSH B was found to be the predominant ovothiol in the hydrozoan *C. hemisphaerica* (Fig. 4B), with a considerably higher abundance than GSH ([OSH]/[GSH] = 3.12).

2.5. OvoA gene expression profiling in Cnidaria

To gather information about a conserved biological role of OSH biosynthesis at the stem of animal evolution, the expression of *ovoA* was analysed in different stages of cnidarian development, including embryos, larvae, and adult phases, exploiting the availability of RNA-seq data from *N. vectensis* (Anthozoa, Actinaria), *M. capitata* (Anthozoa, Scleractinia), and *C. hemisphaerica* (Medusozoa, Hydrozoa). In *N. vectensis*, significant *ovoA* expression was observed in unfertilized eggs, followed by a visible decrease after fertilization, in the zygote and early- and mid-blastula stages (Fig. 5A). Another peak of *ovoA* expression emerged during the gastrula stage and gradually declined in the planula and polyp stages. In adults, *ovoA* was more expressed in females, with barely detectable expression levels in males. In *M. capitata*, *ovoA* mRNA expression was also observed in the eggs, with a slight decrease in the embryo after fertilization (Fig. 5B); these stages were followed by a new surge of *ovoA* expression from the blastula to the prawn chip stages, and a significant increase in the planula. Finally, the expression levels of *ovoA* exhibited great fluctuations throughout development in the hydrozoan *C. hemisphaerica* (Fig. 5C). Three major peaks of gene expression levels were visible, the first starting at the early gastrula to the early planula stage, the second at the gonozoid stage and the third at the

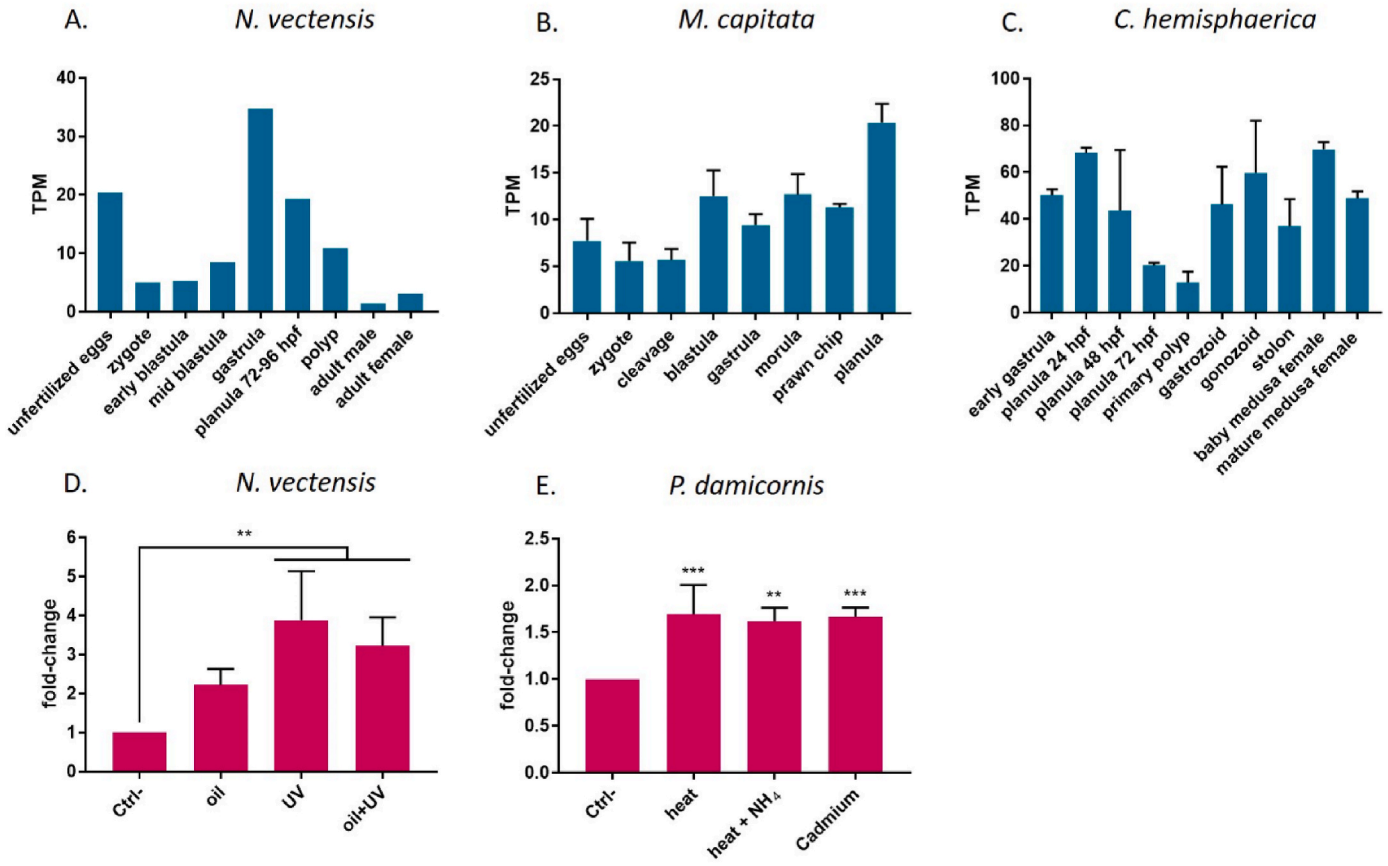

Fig. 5. Comparison of the ovoA expression profiles in the eggs and during the development of the cnidarians. A) *N. vectensis,* B) *M. capitata*, and C) *C. hemisphaerica*. Values are expressed as TPM. OvoA expression profiles in response to environmental stressors. D) weathered oil and UV rays in *N. vectensis* E) heat, ammonium, and cadmium exposure in *P. damicornis.* Values are expressed in fold changes compared to the control using TPM. Data were analysed by One-way ANOVA followed by Dunnett post-test. Bars represent mean ± s.d. ** and *** indicates values significantly higher than ovoA expression level in Ctrl- (** p-value <0.01; *** p-value <0.001).

female baby medusa, with a slight decrease in the mature medusa. This pattern reflects the two distinct life cycles of hydrozoan species. A similar pattern of *ovoA* expression profile is conserved along metazoan evolution (SI Fig. 6), in echinoderms, urochordates, and amphioxus, highlighting the importance of *ovoA* regulation during animal development.

To assess whether OSH biosynthesis could be regulated by external stimuli, the analysis of *ovoA* expression profiles was extended to publicly available RNA-seq data in two anthozoan species exposed to different environmental stressors. A significant overexpression of *ovoA* transcript was observed in adults of *N. vectensis* exposed to weathered oil and ultraviolet (UV) rays [54], compared to the control (Fig. 5D). In the stony coral *P. damicornis,* a pronounced increase in *ovoA* expression levels was observed in coral nubbins exposed to heat stress (32 °C for 24 h) or to a combination of heat and ammonium stress (10 μmol L^{-1}) [55], compared to the control (Hexacorallia, Scleractinia) (Fig. 5E). Furthermore, *P. damicornis* also displayed increased *ovoA* expression levels after heavy metals (Cd) exposure (110 nmol L^{-1}, 12 h) [56].

3. Discussion

Cnidaria are at the crossroads of metazoan evolution and are astonishingly diverse in body form and lifestyle, as exemplified by the jellyfish stage in medusozoans [57]. From an ecological point of view, coral reefs represent a hotspot of biodiversity and an extraordinary reservoir of symbiosis with bacteria and microalgae, whereas jellyfish are the top plankton's predators [7,58]. Some corals and sea anemones lack genes involved in the biosynthesis of amino acids and secondary metabolites, which are provided by microbial symbionts [58]. On the other hand, some corals' genomes have acquired genetic material from algal and bacterial endosymbionts, including genes producing antioxidants and UVR-protective molecules [7,58], while just a limited number of HGT events have been reported in Hydrozoa [59]. However, the molecular machinery that regulates sulfur redox homeostasis and the biosynthesis of secondary metabolites in these basal metazoans is largely unexplored, and its study is expected to provide insights into the evolution of natural products and redox biochemistry control.

This work focused on the almost unexplored molecular machinery involved in OSH biosynthesis, which represents an example of biosynthetic process encoded by animal hosts, challenging the most common view that secondary metabolites in sessile marine animals, such as corals, are mainly produced by bacterial symbionts [60–62]. In this context, OSHs are secondary metabolites produced by marine animals, which are receiving significant attention due to their unique antioxidant and anti-inflammatory properties [14]. In this work, we have recovered *ovoA* sequences from the recently released genomes and transcriptomes of multiple cnidarian species and protists associated with these organisms, performing an in-depth phylogenetic analysis to elucidate the complex evolutionary history of *ovoA* in basal metazoans. We highlighted clear molecular differences between anthozoan and hydrozoan *ovoA* sequences, confirming the presence of genes and proteins with canonical (clade I) structure in the former, and unveiling the presence of peculiar chimaeric *ovoB/ovoA* sequences (clade II) in the latter. These hydrozoan sequences represent unique cases of multidomain proteins within the metazoan lineage combining all three enzymatic activities responsible for OSH biosynthesis in a single polypeptide.

We further investigated the closest relatives to the hydrozoan genes, identifying the most likely source of the HGT event that led to the acquisition of clade II *ovoB/ovoA* sequences in Hydrozoa. Our working hypothesis implies a first *ovoA* gene loss event in the common ancestor of Medusozoa, followed by a re-acquisition in the hydrozoan ancestor by HGT before the split between Trachylinae and Hydroidolina (i.e. 512 Mya), but after the divergence between Hydrozoa and other Medusozoan groups, i.e. 559 Mya [63]. This event is likely to be placed at a time when an ancestral symbiont, living in close association with an ancestor of the hydrozoan lineage, contributed as a donor for the HGT. Intriguingly, the identification of a phylogenetically related sequence in *V. brassicaformis*, a coral-associated apicomplexan parasite belonging to the superphylym Alveolata [64], led us to hypothesize that the chimaeric hydrozoan *ovoB/ovoA* genes were indeed xenologs, acquired through an HGT event from an alveolate symbiont or parasite (Fig. 1B). Nevertheless, the lack of a N-terminal OvoB-like domain in the sequence of *V. brassicaformis* still could not fully explain the chimaeric structure of the hydrozoan genes [11]. The updated results obtained by the *in silico* analysis of available omic resources allowed us to infer with high confidence that the most likely donor source in the HGT event that led to the acquisition of chimaeric *ovoB/ovoA* genes in Hydrozoa was an ancient symbiont/parasite belonging to Alveolata, and most specifically to Syndiniales. This idea is supported by: 1. the placement of the sequences from Hydrozoa and Syndiniales in the same clade by phylogenetic inference; 2. the presence of genes with a shared chimaeric *ovoB/ovoA* architecture in Hydrozoa and Syndiniales, along with the identification of similar sequences in the transcriptomes of other photosynthetic protists that likely host Syndiniales parasites. The presence of these genes in *Amoebophyra*, an endoparasitic dinoflagellate that infects a number of free-living marine dinoflagellates, cnidarians, and some fish, confirmed our hypotheses. Syndiniales are widespread intracellular parasites with a relatively broad host range in marine environments [65], and *Amoebophrya* in particular is frequently associated with dinoflagellates, among other alveolate taxa [66]. As of note, symbioses between dinoflagellates and cnidarians have great ecological importance [67] and, albeit mostly studied in anthozoans, they are also widespread in Hydrozoa [68,69], thereby providing an opportunity for HGT in a context of proximity between an hypothetical gene donor (i.e. a dinoflagellate-associated Syndiniales parasite) and the ancestral hydrozoan host. Moreover, the presence of distinct *ovoA* and *ovoB*-like genes in other Alveolata supports the hypothesis that the two genes were fused at some point during the evolution of Syndiniales, leading to the chimaeric genes observed in *Amoebophrya*. The importance of this ancient HGT event and its contribution to the diversification of OSH metabolic pathway is also emphasized by its persistence to the present day. Intriguingly, we found that the marine hydrozoan *C. hemisphaerica* stands out for its predominant production of OSH B over GSH. Curiously, some photosynthetic protists like the centric and pennate diatoms *S. marinoi* and *P.* tricornutum (belonging to the same clade II) have been recently reported to produce exclusively OSH B [15,70]. This could be a characteristic feature of stramenopiles (heterokonts) and alveolates, which strictly link the world of protists to that of basal animals. Interestingly, *P. tricornutum* strains overexpressing OvoA display a relative decrease of GSH levels [15], suggesting a negative regulation of the two pathways for OSH and GSH production, whose enzymes compete for the same substrate cysteine. Besides presenting the distinctive fusion *ovoB/ovoA* genomic arrangement, hydrozoan sequences also display two SAM domains at the C-terminal position, which are predicted to dimerize in the structural model of the protein from *C. hemisphaerica* (Fig. 2C/F). This type of rearrangement leaves the SAM domains quite flexible and may facilitate the acceptance of previously methylated histidine during OSH B production.

On the other hand, protozoan parasites and human pathogens such as *Leishmania major* and *Trypanosoma cruzi*, and the most closely related *Euglena gracilis*, are known to produce OSH A. According to our theory of an HGT event from an endoparasitic dinoflagellate to hydrozoan species, symbiotic and parasitic interactions have played a key role in the evolution and diversification of thiol species.

The presence of OSHs in basal metazoans had never been reported before this work. The genetic diversity observed through *in silico* genomic and transcriptomic analysis reflected the occurrence of diverse forms of OSHs in cnidarians. We discovered that among Hexacorallia (Anthozoa), the Scleractinia *A. calycularis* produced exclusively OSH A, while the Actinaria *A. equina* produced OSH C, besides GSH. Notably, in the octocoral *E. singularis,* the presence of OSH A and small traces of OSH B, together with the complete absence of GSH, indicate again a negative regulation for the genes involved in GSH biosynthesis. The production of OSH B or OSH C, in addition to OSH A, may be inferred by the promiscuity of OvoA in accepting different methylated histidines, likely available in the environment, as already reported for bacterial *Et*OvoA [71]. However, to date, no homolog of histidine methyltransferase has been identified in animals as cnidarians.

Among Medusozoa, the sessile polyps of *A. aurita* contain GSH but no OSHs, as expected due to the lack of the *ovoA* gene in Scyphozoa. The surprising finding that free-swimming jellyfish stage of both *A. aurita* and *P. noctiluca* species, besides GSH, also contains OSHs inevitably spurs discussions regarding the source of these molecules in adult medusozoans. Alternative hypothesis can be formulated for *ovoA*-lacking organisms, as they may have evolved: 1. membrane transporters to acquire OSHs from the diet, as previously documented for the analogous ERG in humans [72]; 2. symbiotic or parasitic associations with microbial organisms providing OSHs [73]; 3. alternative metabolic strategies to support OSH production. Most likely, *P. noctiluca* acquires OSHs from its diet, which is highly varied thanks to the free-swimming behavior of the adult stage and its appetite for several organisms producing OSHs, such as phytoplankton and mollusks, which are rich in OSH A [74]. The occurrence of OSH A also in the adults of the free-swimming jellyfish *A. aurita,* fed with *A. salina*, suggests that the accumulation of OSHs through the diet is a common trait of the medusa stage.

Finally, we exploited the increasing availability of RNA-seq data for different metazoan species, to comparatively investigate the regulation of *ovoA* transcript during early embryonic development and in response to different environmental stressors in several animal phyla. This comparative *in silico* analysis unveiled a conserved regulation of *ovoA* gene expression in the eggs, embryo, and in different larval stages across a broad taxonomic range (See SI Fig. 5). These data highlighted a conserved role of *ovoA* in safeguarding eggs against excessive ROS production occurring during fertilization and the progression of the correct embryo and larval development in seawater [22,75,76]. Furthermore, the *ovoA* gene regulation observed in coral species upon the exposure to UV and metals is particularly intriguing and may point to the photoprotective and metal chelating properties of OSH. To date, coral-associated photosynthetic symbionts have been considered as key players in the production of mycosporines, photoprotective molecules able to counteract UVA rays reaching seawater and contribute to defense from coral bleaching [77]. To the best of our knowledge, the discovery of OSH biosynthesis in coral animal hosts may represent the first endogenous production of natural products with photoprotective properties in these organisms. Indeed, OSHs display typical antioxidant and UV absorption properties due to the aromaticity of the imidazole ring and the position of the sulphydrylic group [78]. An intriguing aspect is represented by the presence of OSHs in the lenses of fish lacking the *ovoA* gene [79]. Therefore, although OSHs may resemble mycosporine-like amino acids, they would be more widespread due to their origin from a biosynthetic machinery conserved in a broad range of higher eukaryotes.

In conclusion, this study provides novel insights into the evolutionary history and diversification of the molecular players involved in the biosynthesis of OSHs in Cnidaria, contributing to a better understanding of this secondary metabolic pathway across metazoans. The work presented herein provides for the first time evidence of the

biosynthesis of OSHs in cnidarian hosts, enlarging the metabolic complexity of these organisms, and formulate a well-supported hypothesis concerning the genesis and timing of the HGT event that occurred in Hydrozoa.

4. Materials and methods

4.1. Recovery and bioinformatics analysis of cnidarian OvoA amino acid sequences

An updated collection of full-length OvoA protein sequences from cnidarian species was obtained by screening all available de novo assembled genomic and transcriptomic datasets deposited in the NCBI public repositories as of May 2024, using previously identified OvoA sequences [11] as queries for homology searches against the protein nr (using BLASTp), the Whole Genome Shotgun (WGS) and Transcriptome Shotgun Assembly (TSA) sequence databases, using BLASTp and tBLASTn, respectively. Searches, initially carried out using a p-value threshold equal to 1e-5, were restricted to Cnidaria, and all positive matches were manually screened to assess the completeness of sequences and the consistency of domain organization with InterProScan [80], allowing to discriminate genuine OvoA proteins from other related sequences sharing the same domains. Transcripts extracted from TSA were virtually translated using the *translate* tool of Expasy portal [81]. OvoA sequences obtained from genomes lacking annotations were recovered by manually annotating exon sequences based on the combination between sequence homology evidence and computational prediction. In detail, genomic DNA was aligned with transcriptome-derived complementary DNA (cDNA) sequences obtained from the same species, whenever this was available, by Muscle [82] using permissive gap extension parameters (to take into account the presence of introns). Whenever a transcriptome from the same species was unavailable, the cDNA sequence from a phylogenetically closely related species was utilized as a substitute for the alignment and verification process. Errors leading to incorrect predictions of OvoA coding sequences linked with automated gene model annotation processes, such as exon skipping and incorrect splicing sites, were rectified during the manual curation process. Intron and exon boundaries were determined using SPLIGN (https://catalog.data.gov/dataset/splign), and the precise locations of donor and acceptor splicing sites were further refined through the use of GENIE [83], assuming the presence of canonical splicing sites [11]. This process also allowed to reconstruct the architecture of OvoA gene, disregarding the 5′ and 3’ UTR regions, due to the focus placed on coding sequences in this study. A similar approach was used, in non-metazoan organisms, to investigate the presence of sequences similar to those of Hydrozoa. In this case, besides the aforementioned nr protein and WGS/TSA nucleotide databases, sequence homology searches were also carried out against the nucleotide database associated with metagenomes (taxonomy ID 408169), to identify sequences associated with uncharacterized organisms sequenced in the context of environmental sequence analysis. Based on the presence of multiple lineages using non-standard nuclear codes within Alveolata, all matching sequences associated with these organisms were translated using the most appropriate codon tables. All validated full-length protein sequences from non-metazoan species were subjected to pairwise alignments with CD-HIT [84], to reduce redundancy, following the same criteria used in our previous study (i.e. based on a 55 % sequence identity threshold) [11]. To maintain a higher resolution in subsequent analyses, a slightly higher threshold (i.e. 75 %) was used for hydrozoan sequences. All selected sequences were added to the dataset used for the generation of the OvoA phylogenetic tree in our previous study and a multiple sequence alignment (MSA) was generated using Clustal Omega [85]. The MSA was manually refined by removing the N-terminal OvoB-like domain (whenever present) and by trimming all aligned positions characterized by gaps in more than 50 % of the sequences belonging to any of the three previously defined OvoA clades. The resulting trimmed MSA was used as an input for a Maximum Likelihood phylogenetic analysis using IQ-TREE [86], which was run with 1000 ultrafast bootstrap replicates [87] by implementing the best-fitting model of molecular evolution, identified by ModelFinder [88] as LG + I + G4 (a LG model with unequal base frequencies and four rate categories for the discrete gamma distribution of rates among sites [89,90], based on the Bayesian Information Criterion [91]. The tree was graphically represented with FigTree. The conservation of structural domains DinB-like domain (PF12867), FGE-sulfatase domain (PF03781), methyltransferase 11 domain (PF08241) and catalytic residues responsible for OvoA activity were assessed using InterProScan and Clustal Omega tools.

4.2. AlphaFold2 protein modelling

The structure of full length, monomeric OvoBA from *C. hemisphaerica* and of the dimer of the OvoB-like domain were modeled using the Colabfold implementation of AF2, which uses mmseq2 to generate the multi-sequence alignment (MSA) between the primary amino acid sequence of the target proteins and the sequence of homologs as inputs [44,45]. The AF2-ptm and AF2-multimer algorithms were used and 5 models were generated with 3 recycles. Amber minimization was excluded to optimize computational cost. The model of the full length dimer of *Ch*OvoBA was built with AlphaFold3 [48]. Analysis and visualization of the models and figure preparation was realized with ChimeraX [92].

4.3. Transcriptome mining of RNAseq data

The raw RNAseq data deriving from different studies exploiting Illumina paired-end sequencing were obtained by downloading from the NCBI Sequence Read Archive (SRA) database (Supplementary Table 2). The initial raw reads underwent quality assessment and were subsequently trimmed to eliminate sequencing adapters and low-quality bases using fastp version 0.20.0 (Chen 2023). Gene expression levels were calculated as Transcript Per Million (TPM) based on the back-mapping of the original reads to the assembled contigs. This metric ensures the comparability of gene expression levels both within (i.e. among genes) and between samples, since it represents the frequency of transcription of a given gene, assuming the production of a total of 1 million mRNA molecules per biological sample. The presence of authentic *ovoA* sequences in target species was meticulously assessed through a tBLASTn approach, by using previously validated *ovoA* protein sequences as queries. All hits underwent a careful screening to verify the completeness of inferred protein sequences, thanks to the analysis of associated conserved protein domains through InterProScan analysis.

4.4. Cnidarian specimens collection

For the analysis of cellular thiols, cnidarian species with available genomic or transcriptomic data were selected within the Anthozoa class: *Actinia equina*, *Astroides calycularis*, and *Eunicella singularis*. Specimens were collected from Punta Scanella in Ischia island by underwater diving conducted by the SCUBA divers of the Core Facility of the Department of Infrastructure for Marine Research (RIMAR) at SZN. Subsequently, within 1 h from the time of collection, they were carefully transported in insulated containers to the laboratory. In more detail, we analysed, three distinct individuals of *A. equina*, three separate colonies of *A. calycularis* and a small fragment of *E. singularis*. Within the Medusozoa class, we analysed a pool of polyps and a mid-size medusa of *A. aurita*, a pool of 6 young medusae (1 cm in diameter) and two full-grown samples of jellyfish *Pelagia noctiluca*, and a pool of adult medusae of *Clytia hemisphaerica* from the aquarium of Banyuls-sur-Mer, France. Collected samples were lyophilized and freeze-dried tissues were used for thiol qualitative and quantitative analysis.

4.5. Thiols extraction and derivatization

Prior to HPLC and LC-MS analyses, cellular thiols were converted into their BMC-derivatives according to the procedure previously reported [15]. Briefly, 10 mg of freeze-dried and pulverized tissues were rehydrated with 20 μL of water, spiked with 10 μL of 1 mM N-Acetyl-cysteine (NAC) as internal standard, and lysed by extensive vortexing with 90 μL of extraction buffer (Acetonitrile: 0.75 M $HClO_4$, 1: 2 v/v). The samples were centrifuged (5 min, 16000×*g*) to remove insoluble cellular debris and 100 μL of cleared lysate were neutralized by the addition of 15 μL of 2 M K_2CO_3. The mixture was centrifuged (2 min, 16000×*g*) to remove excess potassium perchlorate and 100 μL of supernatant were basified with 10 μL of 50 mM Li_2CO_3. Cellular thiols were reduced with 3 μL of 200 mM DTT (5 min) before adding 25 μL of 20 mM BMC in dimethyl sulfoxide (DMSO) (30 min, in the dark). The mixture was acidified by the addition of 10 μL of 10 % formic acid and vortexed extensively to remove CO_2 and excess BMC before HPLC and LC-MS analysis.

4.6. HPLC and LC-MS analysis

The samples (20 μL) were examined by reversed-phase HPLC utilizing an Agilent Infinity 1260 apparatus equipped with a Poroshell 120-C 18 column (4 μm, 150 × 4.6 mm, Agilent). Detection of thiol-BMC conjugates was accomplished by measuring absorbance at 330 nm. The column was equilibrated with a mixture of 98 % solvent A (0.1 % formic acid in water), and 2 % solvent B (0.1 % formic acid in acetonitrile), at a flow rate of 0.8 mL/min. The following gradient was used: 0.0–2 min, 2 % B; 2.0 min, 3 % B; 2–6min, 3–9% B; 6–21 min, 9–45 % B; 21–23 min, 45–90 % B; 23–26 min, 90 % B; 26–27 min, 90–2% B; 27–34, 2 % B. Standards of 5-thiohistidine, OSH A, GSH, and ERG, were employed to assess the presence or absence of these compounds in the samples. LC-MS analyses were performed on an Agilent ESI-TOF 1260/6230DA instrument, in positive ion mode under the following conditions: nebulizer pressure 35 psig; drying gas (nitrogen) 5 L/min, 325 °C; capillary voltage 3500 V; fragmentor voltage 175 V. An Eclipse Plus C18 column (150 × 4.6 mm, 5 μm) was used, with the same mobile phases as above at a flow rate of 0.4 mL/min to ensure compatibility with the ESI source. The gradient was adjusted to account for the slower flow rate as follows: 0–2 min, 2 % B; 2–6 min, 2–9 % B; 6–24 min, 9–90 % B; 24–29 min, 90 % B; 29–31 min, 90-2 % B; 31–36 min, 2 % B. Thiol identification was conducted by comparing the peaks observed in the MS spectra of the samples with the calculated mass of BMC-alkylated standards, which are reported in Supplementary Table 3, along with their brute formula and observed RT obtained with the gradient used in HPLC and LC-MS, respectively. In the absence of a pure standard for OSH B, we employed the thiol extract from a culture of the engineered diatom *P. tricornutum* overproducing this metabolite [15]. To estimate the ratio between cellular thiols in the different species, OSHs and GSH were quantified based on the area of the corresponding peaks in the HPLC chromatogram, using a calibration curve built with external standards of OSH A and GSH.

CRediT authorship contribution statement

Annalisa Zuccarotto: Writing – original draft, Investigation, Formal analysis, Data curation. **Marco Sollitto:** Investigation, Formal analysis, Data curation. **Lucas Leclère:** Writing – review & editing, Resources, Formal analysis. **Lucia Panzella:** Methodology, Data curation. **Marco Gerdol:** Writing – review & editing, Writing – original draft, Validation, Supervision, Methodology, Investigation, Formal analysis, Data curation, Conceptualization. **Serena Leone:** Writing – review & editing, Supervision, Resources, Methodology, Formal analysis, Data curation, Conceptualization. **Immacolata Castellano:** Writing – review & editing, Writing – original draft, Supervision, Resources, Project administration, Investigation, Funding acquisition, Formal analysis, Data curation, Conceptualization.

Funding

A.Z. has been supported by a PhD fellowship funded by the Stazione Zoologica Anton Dohrn (Open University–Stazione Zoologica Anton Dohrn PhD Program). This research has received funds by the European Union - Next Generation EU, PRIN 2022 awarded by MUR, CUP E53D23009970006.

Acknowledgments

We thank Roberto Arrigoni for his advice on the Cnidaria collection. We thank Anna Palumbo and Florian P. Seebeck for sharing the standards of ovothiol A and 5-thiohistidine, respectively.

Appendix A. Supplementary data

Supplementary data to this article can be found online at https://doi.org/10.1016/j.freeradbiomed.2024.11.037.

References

[1] E. Kayal, B. Roure, H. Philippe, A.G. Collins, D.V. Lavrov, Cnidarian phylogenetic relationships as revealed by mitogenomics, BMC Evolutionary Biology13 5 (2013), https://doi.org/10.1186/1471-2148-13-5.
[2] U. Technau, M. Schwaiger, Recent advances in genomics and transcriptomics of cnidarians, Mar. Genomics 24 (Pt 2) (2015) 131–138.
[3] L. Leclère, C. Horin, S. Chevalier, P. Lapébie, P. Dru, S. Peron, M. Jager, T. Condamine, K. Pottin, S. Romano, et al., The genome of the jellyfish *Clytia hemisphaerica* and the evolution of the cnidarian life-cycle, Nature Ecology & Evolution 3 (2019) 801–810, https://doi.org/10.1038/s41559-019-0833-2.
[4] M.V. Kitahara, H. Fukami, F. Benzoni, D. Huang, The new systematics of scleractinia: integrating molecular and morphological evidence, in: S. Goffredo, Z. Dubinsky (Eds.), The Cnidaria, Past, Present and Future: the World of Medusa and Her Sisters, Springer International Publishing, Cham, 2016, pp. 41–59, https://doi.org/10.1007/978-3-319-31305-4_4.
[5] N.H. Putnam, M. Srivastava, U. Hellsten, B. Dirks, J. Chapman, A. Salamov, A. Terry, H. Shapiro, E. Lindquist, V.V. Kapitonov, et al., Sea anemone genome reveals ancestral eumetazoan gene repertoire and genomic organization, Science 317 (2007) 86–94, https://doi.org/10.1126/science.1139158.
[6] S. Fraune, S. Forêt, A.M. Reitzel, Using Nematostella vectensis to study the interactions between genome, epigenome, and bacteria in a changing environment, Front. Mar. Sci. 3 (2016) 148, https://doi.org/10.3389/fmars.2016.00148.
[7] D. Bhattacharya, S. Agrawal, M. Aranda, S. Baumgarten, M. Belcaid, J.L. Drake, D. Erwin, S. Foret, R.D. Gates, D.F. Gruber, et al., Comparative genomics explains the evolutionary success of reef-forming corals, in: J. Bohlmann (Ed.), Elife 5 (2016) e13288, https://doi.org/10.7554/eLife.13288.
[8] F. Berrue, R.G. Kerr, Diterpenes from gorgonian corals, Nat. Prod. Rep. 26 (2009) 681–710, https://doi.org/10.1039/B821918B.
[9] C. Lyu, T. Chen, B. Qiang, N. Liu, H. Wang, L. Zhang, Z. Liu, CMNPD: a comprehensive marine natural products database towards facilitating drug discovery from the ocean, Nucleic Acids Res. 49 (2021) D509–D515, https://doi.org/10.1093/nar/gkaa763.
[10] I. Burkhardt, T. de Rond, P.Y.-T. Chen, B.S. Moore, Ancient plant-like terpene biosynthesis in corals, Nat. Chem. Biol. 18 (2022) 664–669.
[11] M. Gerdol, M. Sollitto, A. Pallavicini, I. Castellano, The complex evolutionary history of sulfoxide synthase in ovothiol biosynthesis, Proc. Biol. Sci. 286 (2019) 20191812, https://doi.org/10.1098/rspb.2019.1812.
[12] H.S.C. Spies, D.J. Steenkamp, Thiols of intracellular pathogens, Eur. J. Biochem. 224 (1994) 203–213, https://doi.org/10.1111/j.1432-1033.1994.tb20013.x.
[13] R.N. Vogt, H.S.C. Spies, D.J. Steenkamp, The biosynthesis of ovothiol A (N1-methyl-4-mercaptohistidine), Eur. J. Biochem. 268 (2001) 5229–5241. https://onlinelibrary.wiley.com/doi/abs/10.1046/j.0014-2956.2001.02444.x.
[14] I. Castellano, F.P. Seebeck, On ovothiol biosynthesis and biological roles: from life in the ocean to therapeutic potential, Nat. Prod. Rep. 35 (2018) 1241–1250, https://doi.org/10.1039/C8NP00045J.
[15] M.T. Russo, A. Santin, A. Zuccarotto, S. Leone, A. Palumbo, M.I. Ferrante, I. Castellano, The first genetic engineered system for ovothiol biosynthesis in diatoms reveals a mitochondrial localization for the sulfoxide synthase OvoA, Open Biology 13 (2023) 220309, https://doi.org/10.1098/rsob.220309.
[16] G.T.M. Mashabela, F.P. Seebeck, Substrate specificity of an oxygen dependent sulfoxide synthase in ovothiol biosynthesis, Chem. Commun. 49 (2013) 7714–7716, https://doi.org/10.1039/C3CC42594K.
[17] F.P. Seebeck, In vitro reconstitution of Mycobacterial ergothioneine biosynthesis, J. Am. Chem. Soc. 132 (2010) 6632–6633. http://europepmc.org/abstract/MED/20420449.
[18] F.P. Seebeck, Thiohistidine biosynthesis, CHIMIA 67 (2013) 333. https://www.chimia.ch/chimia/article/view/2013_333.

[19] A. Braunshausen, F.P. Seebeck, Identification and characterization of the first ovothiol biosynthetic enzyme, J. Am. Chem. Soc. 133 (6) (2011) 1757–1759. https://api.semanticscholar.org/CorpusID:19593511.
[20] N. Naowarojna, P. Huang, Y. Cai, H. Song, L. Wu, R. Cheng, Y. Li, S. Wang, H. Lyu, L. Zhang, et al., In vitro reconstitution of the remaining steps in ovothiol A biosynthesis: C–S lyase and methyltransferase reactions, Org. Lett. 20 (2018) 5427–5430, https://doi.org/10.1021/acs.orglett.8b02332.
[21] X. Wang, S. Hu, J. Wang, T. Zhang, K. Ye, A. Wen, G. Zhu, A. Vegas, L. Zhang, W. Yan, et al., Biochemical and structural characterization of OvoATh2: a mononuclear nonheme iron enzyme from *Hydrogenimonas thermophila* for ovothiol biosynthesis, ACS Catal. 13 (2023) 15417–15426, https://doi.org/10.1021/acscatal.3c04026.
[22] I. Castellano, O. Migliaccio, S. D'Aniello, A. Merlino, A. Napolitano, A. Palumbo, Shedding light on ovothiol biosynthesis in marine metazoans, Sci. Rep. 6 (2016) 21506, https://doi.org/10.1038/srep21506.
[23] T.P. Holler, P.B. Hopkins, Ovothiols as biological antioxidants. The thiol groups of ovothiol and glutathione are chemically distinct, J. Am. Chem. Soc. 110 (1988) 4837–4838, https://doi.org/10.1021/ja00222a057.
[24] T.P. Holler, P.B. Hopkins, Ovothiols as free-radical scavengers and the mechanism of ovothiol-promoted NAD(P)H-O2 oxidoreductase activity, Biochemistry 29 (1990) 1953–1961, https://doi.org/10.1021/bi00459a042.
[25] E. Turner, R. Klevit, P.B. Hopkins, B.M. Shapiro, Ovothiol: a novel thiohistidine compound from sea urchin eggs that confers NAD(P)H-O2 oxidoreductase activity on ovoperoxidase, J. Biol. Chem. 261 (1986) 13056–13063. https://www.sciencedirect.com/science/article/pii/S0021925818692701.
[26] E. Turner, L.J. Hager, B.M. Shapiro, Ovothiol replaces glutathione peroxidase as a hydrogen peroxide scavenger in sea urchin eggs, Science 242 (1988) 939–941. https://www.science.org/doi/10.1126/science.3187533.
[27] I.K. Cheah, B. Halliwell, Ergothioneine, recent developments, Redox Biol. 42 (2021) 101868. https://www.sciencedirect.com/science/article/pii/S2213231721000161.
[28] B. Halliwell, R.M.Y. Tang, I.K. Cheah, Diet-derived antioxidants: the special case of ergothioneine, Annu. Rev. Food Sci. Technol. 14 (2023) 323–345. https://www.annualreviews.org/content/journals/10.1146/annurev-food-060822-122236.
[29] C. Pathirana, R.J. Andersen, Imbricatine, an unusual benzyltetrahydroisoquinoline alkaloid isolated from the starfish Dermasterias imbricata, J. Am. Chem. Soc. 108 (1986) 8288–8289, https://doi.org/10.1021/ja00286a041.
[30] F. Reyes, R. Martín, A. Rueda, R. Fernández, D. Montalvo, C. Gómez, J.M. Sánchez-Puelles, Discorhabdins I and L, cytotoxic alkaloids from the sponge Latrunculia brevis, J. Nat. Prod. 67 (2004) 463–465, https://doi.org/10.1021/np0303761.
[31] J.P. Torres, Z. Lin, M. Watkins, P.F. Salcedo, R.P. Baskin, S. Elhabian, H. Safavi-Hemami, D. Taylor, J. Tun, G.P. Concepcion, et al., Small-molecule mimicry hunting strategy in the imperial cone snail, *Conus imperialis*, Sci. Adv. 7 (2021) eabf2704. https://europepmc.org/articles/PMC7954447.
[32] I. Castellano, P. DiTomo, N. DiPietro, D. Mandatori, C. Pipino, G. Formoso, A. Napolitano, A. Palumbo, A. Pandolfi, Anti-inflammatory activity of marine ovothiol a in an in vitro model of endothelial dysfunction induced by hyperglycemia, Oxid. Med. Cell. Longev. 2018 (2018). https://doi.org/10.1155/2018/2087373.
[33] M. Brancaccio, G. D'Argenio, V. Lembo, A. Palumbo, I. Castellano, Antifibrotic effect of marine ovothiol in an in vivo model of liver fibrosis, Oxid. Med. Cell. Longev. 2018 (2018). https://doi.org/10.1155/2018/5045734.
[34] M. Brancaccio, M. Russo, M. Masullo, A. Palumbo, G.L. Russo, I. Castellano, Sulfur-containing histidine compounds inhibit γ-glutamyl transpeptidase activity in human cancer cells, J. Biol. Chem. 294 (2019) 14603–14614, https://doi.org/10.1074/jbc.RA119.009304.
[35] M. Brancaccio, A. Milito, C.A. Viegas, A. Palumbo, D.C. Simes, I. Castellano, First evidence of dermo-protective activity of marine sulfur-containing histidine compounds, Free Radic. Biol. Med. 192 (2022) 224–234. https://www.sciencedirect.com/science/article/pii/S0891584922005998.
[36] J.F. Cazet, S. Siebert, H.M. Little, P. Bertemes, A.S. Primack, P. Ladurner, M. Achrainer, M.T. Fredriksen, R.T. Moreland, S. Singh, et al., A chromosome-scale epigenetic map of the *Hydra* genome reveals conserved regulators of cell state, Genome Res. 33 (2023) 283–298. http://europepmc.org/abstract/MED/36639202.
[37] M. Hamada, N. Satoh, K. Khalturin, A reference genome from the symbiotic Hydrozoan, Hydra viridissima. G3 Genes|Genomes|Genetics 10 (2020) 3883–3895, https://doi.org/10.1534/g3.120.401411.
[38] Y. Hasegawa, T. Watanabe, R. Otsuka, S. Toné, S. Kubota, H. Hirakawa, Genome assembly and transcriptomic analyses of the repeatedly rejuvenating jellyfish Turritopsis dohrnii, DNA Res. 30 (2023) dsac047, https://doi.org/10.1093/dnares/dsac047.
[39] K. Kon-Nanjo, T. Kon, H.R. Horkan, Febrimarsa, R.E. Steele, P. Cartwright, U. Frank, O. Simakov, Chromosome-level genome assembly of Hydractinia symbiolongicarpus, G3 Genes|Genomes|Genetics 13 (2023) jkad107, https://doi.org/10.1093/g3journal/jkad107.
[40] M. Pascual-Torner, D. Carrero, J.G. Pérez-Silva, D. Álvarez-Puente, D. Roiz-Valle, G. Bretones, D. Rodríguez, D. Maeso, E. Mateo-González, Y. Español, et al., Comparative genomics of mortal and immortal cnidarians unveils novel keys behind rejuvenation, Proc Natl Acad Sci U S A. 119 (2022) e2118763119. http://europepmc.org/abstract/MED/36037356.
[41] A. Török, P.H. Schiffer, C.E. Schnitzler, K. Ford, J.C. Mullikin, A.D. Baxevanis, A. Bacic, U. Frank, S.G. Gornik, The cnidarian *Hydractinia echinata* employs canonical and highly adapted histones to pack its DNA, Epigenet. Chromatin 9 (2016) 36, https://doi.org/10.1186/s13072-016-0085-1.
[42] E. Kayal, B. Bentlage, Pankey M. Sabrina, A.H. Ohdera, M. Medina, D.C. Plachetzki, A.G. Collins, J.F. Ryan, Phylogenomics provides a robust topology of the major cnidarian lineages and insights on the origins of key organismal traits, BMC Evol. Biol. 18 (2018) 68, https://doi.org/10.1186/s12862-018-1142-0.
[43] L. Chen, N. Naowarojna, H. Song, S. Wang, J. Wang, Z. Deng, C. Zhao, P. Liu, Use of a tyrosine analogue to modulate the two activities of a nonheme iron enzyme OvoA in ovothiol biosynthesis, cysteine oxidation versus oxidative C–S bond formation, J. Am. Chem. Soc. 140 (2018) 4604–4612, https://doi.org/10.1021/jacs.7b13628.
[44] J. Jumper, R. Evans, A. Pritzel, T. Green, M. Figurnov, O. Ronneberger, K. Tunyasuvunakool, R. Bates, A. Žídek, A. Potapenko, et al., Highly accurate protein structure prediction with AlphaFold, Nature 596 (2021) 583–589, https://doi.org/10.1038/s41586-021-03819-2.
[45] M. Mirdita, K. Schütze, Y. Moriwaki, L. Heo, S. Ovchinnikov, M. Steinegger, ColabFold: making protein folding accessible to all, Nat. Methods 19 (2022) 679–682, https://doi.org/10.1038/s41592-022-01488-1.
[46] K.M. Ruff, R.V. Pappu, AlphaFold and implications for intrinsically disordered proteins, J. Mol. Biol. 433 (2021) 167208. https://www.sciencedirect.com/science/article/pii/S0022283621004411.
[47] J. Liang, Q. Han, Y. Tan, H. Ding, J. Li, Current advances on structure-function relationships of pyridoxal 5′-phosphate-dependent enzymes, Front. Mol. Biosci. 6 (2019). https://www.frontiersin.org/articles/10.3389/fmolb.2019.00004.
[48] J. Abramson, J. Adler, J. Dunger, R. Evans, T. Green, A. Pritzel, O. Ronneberger, L. Willmore, A.J. Ballard, J. Bambrick, et al., Accurate structure prediction of biomolecular interactions with AlphaFold 3, Nature 630 (2024) 493–500, https://doi.org/10.1038/s41586-024-07487-w.
[49] S. Farhat, P. Le, E. Kayal, B. Noel, E. Bigeard, E. Corre, F. Maumus, I. Florent, A. Alberti, J.-M. Aury, et al., Rapid protein evolution, organellar reductions, and invasive intronic elements in the marine aerobic parasite dinoflagellate Amoebophrya spp, BMC Biol. 19 (2021) 1, https://doi.org/10.1186/s12915-020-00927-9.
[50] U. John, Y. Lu, S. Wohlrab, M. Groth, J. Janouškovec, S. Kohli Gurjeet, F.C. Mark, U. Bickmeyer, S. Farhat, M. Felder, et al., An aerobic eukaryotic parasite with functional mitochondria that likely lacks a mitochondrial genome, Sci. Adv. 5 (2019) eaav1110. http://europepmc.org/abstract/MED/31032404.
[51] A.L. Mitchell, M. Scheremetjew, H. Denise, S. Potter, A. Tarkowska, M. Qureshi, G. A. Salazar, S. Pesseat, M.A. Boland, F.M.I. Hunter, et al., EBI Metagenomics in 2017: enriching the analysis of microbial communities, from sequence reads to assemblies, Nucleic Acids Res. 46 (2018) D726–D735, https://doi.org/10.1093/nar/gkx967.
[52] A. Ciancio, S. Scippa, M. Finetti-Sialer, A. De Candia, B. Avallone, M. De Vincentiis, Redescription of *Cardiosporidium cionae* (van gaver and stephan, 1907) (apicomplexa: piroplasmida), a plasmodial parasite of ascidian haemocytes, Eur. J. Protistol. 44 (2008) 181–196. https://www.sciencedirect.com/science/article/pii/S0932473907000752.
[53] M.B. Saffo, A.M. McCoy, C. Rieken, C.H. Slamovits, Nephromyces, a beneficial apicomplexan symbiont in marine animals, Proc. Natl. Acad. Sci. USA 107 (2010) 16190–16195, https://doi.org/10.1073/pnas.1002335107.
[54] A.M. Tarrant, S.L. Payton, A.M. Reitzel, D.T. Porter, M.J. Jenny, Ultraviolet radiation significantly enhances the molecular response to dispersant and sweet crude oil exposure in *Nematostella vectensis*, Mar. Environ. Res. 134 (2018) 96–108. https://www.sciencedirect.com/science/article/pii/S0141113617305251.
[55] X. Yu, B. Huang, Z. Zhou, J. Tang, Y. Yu, Involvement of caspase3 in the acute stress response to high temperature and elevated ammonium in stony coral *Pocillopora damicornis*, Gene 637 (2017) 108–114. https://www.sciencedirect.com/science/article/pii/S0378111917307746.
[56] Z. Zhou, X. Yu, J. Tang, Y. Wu, L. Wang, B. Huang, Systemic response of the stony coral *Pocillopora damicornis* against acute cadmium stress, Aquat. Toxicol. 194 (2018) 132–139. https://www.sciencedirect.com/science/article/pii/S0166445X17303399.
[57] K. Khalturin, C. Shinzato, M. Khalturina, M. Hamada, M. Fujie, R. Koyanagi, M. Kanda, H. Goto, F. Anton-Erxleben, M. Toyokawa, et al., Medusozoan genomes inform the evolution of the jellyfish body plan, Nature Ecology & Evolution 3 (2019) 811–822, https://doi.org/10.1038/s41559-019-0853-y.
[58] S. Baumgarten, O. Simakov, L.Y. Esherick, Y.J. Liew, E.M. Lehnert, C.T. Michell, Y. Li, E.A. Hambleton, A. Guse, M.E. Oates, et al., The genome of *Aiptasia*, a sea anemone model for coral symbiosis, Proc. Natl. Acad. Sci. USA 112 (2015) 11893–11898. https://www.pnas.org/doi/full/10.1073/pnas.1513318112.
[59] J.A. Chapman, E.F. Kirkness, O. Simakov, S.E. Hampson, T. Mitros, T. Weinmaier, T. Rattei, P.G. Balasubramanian, J. Borman, D. Busam, et al., The dynamic genome of *Hydra*, Nature 464 (2010) 592–596, https://doi.org/10.1038/nature08830.
[60] M.C. Wilson, T. Mori, C. Rückert, A.R. Uria, M.J. Helf, K. Takada, C. Gernert, U.A. E. Steffens, N. Heycke, S. Schmitt, et al., An environmental bacterial taxon with a large and distinct metabolic repertoire, Nature 506 (2014) 58–62. https://www.nature.com/articles/nature12959.
[61] T.E. Smith, C.D. Pond, E. Pierce, Z.P. Harmer, J. Kwan, M.M. Zachariah, M. K. Harper, T.P. Wyche, T.K. Matainaho, T.S. Bugni, et al., Accessing chemical diversity from the uncultivated symbionts of small marine animals, Nat. Chem. Biol. 14 (2018) 179–185, https://doi.org/10.1038/nchembio.2537.
[62] J.P. Torres, E.W. Schmidt, The biosynthetic diversity of the animal world, J. Biol. Chem. 294 (2019) 17684–17692. https://www.jbc.org/article/S0021-9258(20)30756-0/abstract.
[63] S. Kumar, M. Suleski, J.M. Craig, A.E. Kasprowicz, M. Sanderford, M. Li, G. Stecher, S.B. Hedges, TimeTree 5: an expanded resource for species divergence times, Mol. Biol. Evol. 39 (2022) msac174, https://doi.org/10.1093/molbev/msac174.
[64] M. Oborník, D. Modrý, M. Lukeš, E. Cernotíková-Stříbrná, J. Cihlář, M. Tesařová, E. Kotabová, M. Vancová, O. Prášil, J. Lukeš, Morphology, ultrastructure and life

cycle of Vitrella brassicaformis n. sp., n. gen., a novel chromerid from the Great Barrier Reef, Protist 163 (2012) 306–323. http://europepmc.org/abstract/MED/22055836.
[65] L. Guillou, M. Viprey, A. Chambouvet, R.M. Welsh, A.R. Kirkham, R. Massana, D. J. Scanlan, A.Z. Worden, Widespread occurrence and genetic diversity of marine parasitoids belonging to Syndiniales (Alveolata), Environ. Microbiol. 10 (2008) 3349–3365, https://doi.org/10.1111/j.1462-2920.2008.01731.x.
[66] M.G. Park, W. Yih, D.W. Coats, Parasites and phytoplankton, with special emphasis on dinoflagellate Infections1, J. Eukaryot. Microbiol. 51 (2004) 145–155, https://doi.org/10.1111/j.1550-7408.2004.tb00539.x.
[67] K. Davy Simon, Denis Allemand, Virginia M. Weis, Cell Biology of Cnidarian-dinoflagellate symbiosis, Microbiol. Mol. Biol. Rev. 76 (2012) 229–261, https://doi.org/10.1128/mmbr.05014-11.
[68] T.C. LaJeunesse, W.K.W. Loh, R. van Woesik, O. Hoegh-Guldberg, G.W. Schmidt, W.K. Fitt, Low symbiont diversity in southern Great Barrier Reef corals, relative to those of the Caribbean, Limnol. Oceanogr. 48 (2003) 2046–2054, https://doi.org/10.4319/lo.2003.48.5.2046.
[69] R.K. Trench, R.J. Blank, *Symbiodinium microadriaticum freudenthal, S. Goreauii sp. Nov., S. Kawagutii sp. Nov. And S. Pilosum sp.* Nov.: gymnodinioid dinoflagellate symbionts of marine invertebrates 1, J. Phycol. 23 (1987) 469–481. https://onlinelibrary.wiley.com/doi/abs/10.1111/j.1529-8817.1987.tb02534.x.
[70] A. Milito, I. Castellano, R. Burn, F.P. Seebeck, C. Brunet, A. Palumbo, First evidence of ovothiol biosynthesis in marine diatoms, Free Radic. Biol. Med. 152 (2020) 680–688. https://www.sciencedirect.com/science/article/pii/S0891584919323718.
[71] H. Song, M. Leninger, N. Lee, P. Liu, Regioselectivity of the oxidative C–S bond formation in ergothioneine and ovothiol biosyntheses, Org. Lett. 15 (2013) 4854–4857, https://doi.org/10.1021/ol402275t.
[72] D. Gründemann, S. Harlfinger, S. Golz, A. Geerts, A. Lazar, R. Berkels, N. Jung, A. Rubbert, E. Schömig, Discovery of the ergothioneine transporter, Proc. Natl. Acad. Sci. USA 102 (2005) 5256–5261, https://doi.org/10.1073/pnas.0408624102.
[73] M. Brancaccio, M. Tangherlini, R. Danovaro, I. Castellano, Metabolic adaptations to marine environments: molecular diversity and evolution of ovothiol biosynthesis in bacteria, Genome Biology and Evolution 13 (2021) evab169, https://doi.org/10.1093/gbe/evab169.
[74] U. Tilves, J.E. Purcell, V.L. Fuentes, A. Torrents, M. Pascual, V. Raya, J.-M. Gili, A. Sabatés, Natural diet and predation impacts of *Pelagia noctiluca* on fish eggs and larvae in the NW Mediterranean, J. Plankton Res. 38 (2016) 1243–1254, https://doi.org/10.1093/plankt/fbw059.
[75] B.M. Shapiro, The control of oxidant stress at fertilization, Science 252 (1991) 533–536, https://doi.org/10.1126/science.1850548.
[76] A. Milito, M. Cocurullo, A. Columbro, S. Nonnis, G. Tedeschi, I. Castellano, M. I. Arnone, A. Palumbo, Ovothiol ensures the correct developmental programme of the sea urchin *Paracentrotus lividus* embryo, Open Biology 12 (2022) 210262, https://doi.org/10.1098/rsob.210262.
[77] P.K. Lawrence, F.P. Long, R.A. Young, Mycosporine-like amino acids for skin photoprotection, Curr. Med. Chem. 25 (2018) 5512–5527. http://www.eurekaselect.com/article/83732.
[78] A. Luccarini, A. Zuccarotto, R. Galeazzi, C. Morresi, M. Masullo, I. Castellano, E. Damiani, Insights on the UV-screening potential of marine-inspired thiol compounds, Mar. Drugs 22 (2023) 2.
[79] V.V. Yanshole, L.V. Yanshole, E.A. Zelentsova, Y.P. Tsentalovich, Ovothiol A is the main antioxidant in fish lens, Metabolites 9 (2019) 95. https://www.mdpi.com/2218-1989/9/5/95.
[80] P. Jones, D. Binns, H.-Y. Chang, M. Fraser, W. Li, C. McAnulla, H. McWilliam, J. Maslen, A. Mitchell, G. Nuka, et al., InterProScan 5: genome-scale protein function classification, Bioinformatics 30 (2014) 1236–1240. http://europepmc.org/abstract/MED/24451626.
[81] E. Gasteiger, A. Gattiker, C. Hoogland, I. Ivanyi, R.D. Appel, A. Bairoch, ExPASy: the proteomics server for in-depth protein knowledge and analysis, Nucleic Acids Res. 31 (2003) 3784–3788, https://doi.org/10.1093/nar/gkg563.
[82] R.C. Edgar, MUSCLE: multiple sequence alignment with high accuracy and high throughput, Nucleic Acids Res. 32 (2004) 1792–1797, https://doi.org/10.1093/nar/gkh340.
[83] S.E. Cooper, J. Schwartzentruber, E. Bello, E.L. Coomber, A.R. Bassett, Screening for functional transcriptional and splicing regulatory variants with GenIE, Nucleic Acids Res. 48 (2020) e131, https://doi.org/10.1093/nar/gkaa960.
[84] W. Li, A. Godzik, Cd-hit: a fast program for clustering and comparing large sets of protein or nucleotide sequences, Bioinformatics 22 (2006) 1658–1659, https://doi.org/10.1093/bioinformatics/btl158.
[85] F. Sievers, D.G. Higgins, Clustal Omega for making accurate alignments of many protein sequences, Protein Sci. 27 (2018) 135–145, https://doi.org/10.1002/pro.3290.
[86] L.-T. Nguyen, H.A. Schmidt, A. von Haeseler, B.Q. Minh, IQ-TREE: a fast and effective stochastic algorithm for estimating maximum-likelihood phylogenies, Mol. Biol. Evol. 32 (2015) 268–274, https://doi.org/10.1093/molbev/msu300.
[87] B.Q. Minh, M.A.T. Nguyen, A. von Haeseler, Ultrafast approximation for phylogenetic bootstrap, Mol. Biol. Evol. 30 (2013) 1188–1195, https://doi.org/10.1093/molbev/mst024.
[88] S. Kalyaanamoorthy, B.Q. Minh, T.K.F. Wong, A. von Haeseler, L.S. Jermiin, ModelFinder: fast model selection for accurate phylogenetic estimates, Nat. Methods 14 (2017) 587–589, https://doi.org/10.1038/nmeth.4285.
[89] S.Q. Le, O. Gascuel, An improved general amino acid replacement matrix, Mol. Biol. Evol. 25 (2008) 1307–1320, https://doi.org/10.1093/molbev/msn067.
[90] Z. Yang, Maximum likelihood phylogenetic estimation from DNA sequences with variable rates over sites: approximate methods, J. Mol. Evol. 39 (1994) 306–314.
[91] A.A. Neath, J.E. Cavanaugh, The Bayesian information criterion: background, derivation, and applications, WIREs Computational Statistics 4 (2012) 199–203, https://doi.org/10.1002/wics.199.
[92] E.C. Meng, T.D. Goddard, E.F. Pettersen, G.S. Couch, Z.J. Pearson, J.H. Morris, T. E. Ferrin, UCSF ChimeraX: tools for structure building and analysis, Protein Sci. 32 (2023) e4792, https://doi.org/10.1002/pro.4792.